The Journal of Neuroscience, December 1, 1997, 17(23):9212–9219

Glutamate Transporter GLAST Is Expressed in the Radial Glia–Astrocyte Lineage of Developing Mouse Spinal Cord

Takashi Shibata,[1,2] Keiko Yamada,[1] Masahiko Watanabe,[1] Kazuhiro Ikenaka,[3] Keiji Wada,[4] Kohichi Tanaka,[4] and Yoshiro Inoue[1]

Departments of [1]Anatomy and [2]Urology, Hokkaido University School of Medicine, Sapporo 060, Japan, [3]National Institute for Physiological Sciences, Okazaki National Research Institutes, Okazaki 444, Japan, and [4]Department of Degenerative Neurological Diseases, National Institute of Neuroscience, National Center of Neurology and Psychiatry, Kodaira 187, Japan

The glutamate transporter GLAST is localized on the cell membrane of mature astrocytes and is also expressed in the ventricular zone of developing brains. To characterize and follow the GLAST-expressing cells during development, we examined the mouse spinal cord by *in situ* hybridization and immunohistochemistry. At embryonic day (E) 11 and E13, cells expressing GLAST mRNA were present only in the ventricular zone, where GLAST immunoreactivity was associated with most of the cell bodies of neuroepithelial cells. In addition, GLAST immunoreactivity was detected in radial processes running through the mantle and marginal zones. From this characteristic cytology, GLAST-expressing cells at early stages were judged to be radial glia cells. At E15, cells expressing GLAST mRNA first appeared in the mantle zone, and GLAST-immunopositive punctate or reticular protrusions were formed along the radial processes. From E18 to postnatal day (P) 7, GLAST mRNA or its immunoreactivity gradually decreased from the ventricular zone and disappeared from radial processes, whereas cells with GLAST mRNA spread all over the mantle zone and GLAST-immunopositive punctate/reticular protrusions predominated in the neuropils. At P7, GLAST-expressing cells were immunopositive for glial fibrillary acidic protein, an intermediate filament specific to astrocytes. Therefore, the glutamate transporter GLAST is expressed from radial glia through astrocytes during spinal cord development. Furthermore, the distinct changes in the cell position and morphology suggest that both the migration and transformation of radial glia cells begin in the spinal cord between E13 and E15, when the active stage of neuronal migration is over.

Key words: glutamate transporter; GLAST; radial glia; astrocyte; spinal cord; development; in situ *hybridization; immunohistochemistry; mouse*

Glutamate is a major neurotransmitter mediating the fast excitatory transmission at central synapses, and it also plays critical roles in synaptic plasticity and development (Mayer and Westbrook, 1987). The extracellular glutamate concentration has to be kept low enough to terminate glutamate receptor activation and to protect neurons from glutamate excitotoxicity (Hertz, 1979; Choi, 1992; Tanaka K et al., 1997). The low extracellular concentration is attributable to the action of high-affinity, sodium-dependent glutamate transporters. Molecular biological studies have identified four subtypes of the glutamate transporter with distinct structures, functions, and distributions (Kanai et al., 1997). In the brain, GLAST (GluT-1 or EAAT1) and GLT1 (EAAT2) are the astrocytic transporters, being highly concentrated in the cerebellum and the telencephalon, respectively (Kanai and Hediger, 1992; Storck et al., 1992; Rothstein et al., 1994; Torp et al., 1994; Lehre et al., 1995; Shibata et al., 1996). On the other hand, EAAC1 (EAAT3) and EAAT4 are the neuronal transporters; the former is expressed widely in the brain (Kanai et al., 1995; Kiryu et al., 1995; Shibata et al., 1996), whereas the latter expression is confined to cerebellar Purkinje cells (Yamada et al., 1996). Immunoelectron microscopy has clarified that GLAST and GLT1 are more abundant on astrocytic cell membrane that surrounds synapses than that facing dendritic shafts, vessels, pial surface, and neighboring astrocytes (Chaudhry et al., 1995). EAAT4 is selectively localized at the extrajunctional site of Purkinje cell spines contacting parallel fibers or climbing fibers (Yamada et al., 1996; Tanaka J et al., 1997). The preferential and highly regulated localizations at synaptic regions provide a molecular–anatomical basis for glutamate transporter function in rapid removal of glutamate or its related amino acids from the synaptic cleft.

Four glutamate transporter subtypes also exhibit distinct expression and distribution in the fetal brain, even before synaptogenesis (Shibata et al., 1996; Sutherland et al., 1996; Yamada et al., 1997). Of these, GLAST is characterized by prominent expression of the mRNA in the ventricular zone of various brain regions, a transient zone that produces most neurons and neuroglia. The expression of GLAST mRNA from early stages suggests that the glutamate transporter is involved not only in the regulation of synaptic transmission, but it also plays some role in the development and differentiation of the CNS. As the first step to test this possibility, we attempted to characterize and follow cells expressing GLAST. In the present study, we examined the developing mouse spinal cord by taking advantage of its simple tube-like structure throughout development and of well documented histogenesis and cytogenesis (Choi, 1981; Altman and Bayer,

Received June 19, 1997; revised Sept. 11, 1997; accepted Sept. 19, 1997.

This investigation was supported in part by grants-in-aid for Scientific Research on Priority Areas from the Ministry of Education, Science, Sports, and Culture of Japan and also by research grants from the Ministry of Health and Welfare of Japan, the Science and Technology Agency of Japan, the Suhara Foundation, and the Ichiro Kanehara Foundation. We thank Dr. Yasuhiro Tomooka at the Science University of Tokyo for his kind gift of rabbit anti-nestin antibody, and also Mr. Hideo Umeda and Mr. Yoshihiko Ogawa at the Hokkaido University School of Medicine for their technical assistance.

T.S. and K.Y. contributed equally to this work.

Correspondence should be addressed to Masahiko Watanabe, Department of Anatomy, Hokkaido University School of Medicine, Sapporo 060, Japan.

Copyright © 1997 Society for Neuroscience 0270-6474/97/179212-08$05.00/0

1984). Here we show that GLAST is expressed in the radial glia–astrocyte lineage in the developing spinal cord. Furthermore, characteristic temporal changes in the cell position and morphology, as visualized by *in situ* hybridization and immunohistochemistry for GLAST, suggest that both the migration and transformation of radial glia cells begin at a specific stage of development.

MATERIALS AND METHODS

Animals and tissues. In the present study, we used the lumbar spinal cord of C57BL/6J mice at embryonic day (E) 9, E11, E13, E15, and E18, postnatal day (P) 1, P7, P14, and P21, and 4 months (adult) as well as the adult brain. The day after overnight mating was counted as E0. For isotopic *in situ* hybridization, fresh frozen tissues were prepared from mice at E11 through the adult stage under deep pentobarbital anesthesia. For histological examination, immunohistochemistry, and nonisotopic *in situ* hybridization, fetuses from E9 to E18 were immersed overnight in the Bouin fixative at 4°C, and postnatal mice were perfused transcardially with 4% paraformaldehyde in 0.1 M sodium phosphate buffer, pH 7.2.

Histology. Cross sections (5 μm) were prepared from the spinal cord, embedded in paraffin wax, and stained with hematoxylin. From five sections, the mean number of nuclear profiles per single sections was calculated for the ventricular or mantle zone.

In situ *hybridization.* For isotopic detection of the mouse GLAST mRNA, two nonoverlapping antisense 45-mer oligonucleotide probes were labeled with ^{35}S-dATP using terminal deoxyribonucleotidyl transferase (BRL, Bethesda, MD) to a specific activity of 0.5×10^9 dpm/μg DNA. The probe sequence was complementary to nucleotide residues 11–56 or 669–714 of the mouse GLAST cDNA (Tanaka, 1993). Fresh frozen sections (20 μm in thickness) were treated at room temperature with the following incubations: fixation with 4% paraformaldehyde for 10 min, acetylation with 0.25% acetic anhydride in 0.1 M triethanolamine-HCl, pH 8.0, for 10 min, and prehybridization for 1 hr in a buffer containing 50% formamide, 50 mM Tris-HCl, pH 7.5, 0.02% Ficoll, 0.02% polyvinylpyrrolidone, 0.02% bovine serum albumin, 0.6 M NaCl, 0.25% SDS, 200 μg/ml tRNA, 1 mM EDTA, and 10% dextran sulfate. Hybridization was performed at 42°C for 10 hr in the prehybridization buffer supplemented with 10,000 cpm/μl of ^{35}S-labeled oligonucleotide probes and 0.1 M dithiothreitol. The slides were washed twice at 55°C for 40 min in 0.1 × SSC containing 0.1% sarcosyl and exposed to either Hyperfilm-β max (Amersham, Arlington Heights, IL) or nuclear track emulsion (Kodak NTB-2, Rochester, NY).

For nonisotopic detection, digoxigenin (DIG)-labeled sense and antisense cRNA probes were prepared, using linearized Bluescript SK (−) plasmid containing a 733 base pair cDNA fragment corresponding to nucleotide residues 1746–2478 (Tanaka, 1993). The transcribed cRNAs were alkali-digested to an average length of 150 bases. Procedures for nonisotopic *in situ* hybridization were the same as for isotopic hybridization, except that paraffin sections were partially digested, before fixation, with 100 μg/ml of pepsin (Dako, Carpinteria, California) in 0.2 N HCl for 10 min at 37°C and hybridization was performed at 50°C. The hybridization reaction was visualized using DIG Nucleic Acid Detection Kit (Boehringer Mannheim, Mannheim, Germany).

Antibody preparation. To produce GLAST-specific antibody, an amino acid sequence (KKPYQLIAQDNEPEKPVADSETKM) corresponding to the C terminus of the mouse GLAST (Tanaka, 1993) was synthesized. A cysteine residue was introduced at the C terminus of the synthetic peptide, to facilitate the conjugation to keyhole limpet hemocyanin (KLH) with the 3-maleidobenzoic acid *N*-hydroxy succinimide ester (MBS) methods. The peptide/KLH conjugates emulsified with Freund's complete adjuvant (Difco, Detroit, MI) were injected subcutaneously into a New Zealand White rabbit or a guinea pig at intervals of 2–4 weeks. Two weeks after the last injection, the IgG fraction was purified from the antiserum, using Protein G Sepharose (Pharmacia Biotec AB, Uppsala, Sweden). The peptide-specific IgG was affinity-purified, using CNBr-activated Sepharose 4B (Pharmacia Biotech AB).

Immunoblot. Membrane extracts from the mouse forebrain and cerebellum were prepared by homogenization in 8–10 vol of ice-cold buffer containing 250 mM sucrose, 25 mM KCl, 50 mM Tris-HCl, pH 7.5, and 4 mM $MgCl_2$, using a Potter homogenizer with 15 strokes at 800 rpm. Protein concentration of the supernatants after $1000 \times g$ centrifugation for 10 min was determined by Lowry's method. Ten micrograms of the protein samples were analyzed on an 11% SDS-polyacrylamide gel under reducing conditions. Proteins in the gel were electroblotted onto a nitrocellulose membrane (Schleicher & Schuell, Dassel, Germany). The membrane was incubated with affinity-purified GLAST antibody at a concentration of 1 μg/ml in PBS containing 0.1% Tween 20 and 5% skim milk and visualized with an ECL chemiluminescence detection system (Amersham).

Immunohistochemistry. For immunoperoxidase staining, paraffin or microslicer sections (50 μm) were incubated overnight with the rabbit anti-GLAST antibody at a concentration of 0.1–0.25 μg/ml at room temperature and further incubated with biotinylated second antibodies for 1 hr and avidin–biotin–peroxidase complex for 30 min (Histofine SAB-PO(R) kit, Nichirei, Tokyo, Japan). Immunoreaction was visualized with 3,3′-diaminobenzidine. After nonisotopic *in situ* hybridization, some sections were processed for immunoperoxidase staining with rabbit anti-glial fibrillary acid protein (GFAP) antibody (1:10; Dako).

For double-labeling immunofluorescence, paraffin sections were incubated overnight at room temperature with guinea pig anti-GLAST antibody (2.5 μg/ml) and with rabbit anti-nestin antibody (1:500) (Tomooka et al., 1993), rabbit anti-GFAP antibody (1:1), or rabbit anti-synaptophysin antibody (1:200) (Biotechnik, Heidelberg, Germany), respectively. Immunoreaction by the guinea pig antibody was visualized with biotinylated goat anti-guinea pig IgG for 2 hr (1:500) (Jackson ImmunoResearch, West Grove, PA) and streptavidin–Texas Red for 30 min (10 μg/ml) (Vector, Burlingame, CA), whereas that by the rabbit antibodies was visualized with FITC-labeled donkey anti-rabbit IgG for 2 hr (1:200). Some sections were counterstained with 10 μM propidium iodide (Molecular Probes, Eugene, OR). Sections were photographed by a confocal laser scanning microscope (MRC 1024, Bio-Rad, Hercules, CA).

RESULTS

General histology

Cross sections of developing mouse spinal cords were histologically examined by hematoxylin (Fig. 1). At E9, a large lumen of the central canal was encompassed, with the neural wall consisting of lateral plates, floor plate, and roof plate (Fig. 1*A*). At this stage, the lateral plate was occupied exclusively by the ventricular zone, whereas the mantle and marginal zones were not clearly recognized (Fig. 1*B*). At E11, thin mantle and marginal zones appeared between the ventricular zone and pial surface (Fig. 1*C*). The mantle zone in the ventral cord was observed as the ventral horn, a small oval bulging in the ventrolateral portion (Fig. 1*D*). At E13, the thickness of the ventricular zone was reduced to a two- to three-cell-thick layer, whereas the mantle zone in the ventral and dorsal cords was expanded (Fig. 1*E,F*). In the dorsal cord, a cell-dense layer transiently appeared between the ventricular zone and dorsal horn (*arrowheads* in Fig. 1*E*). At E15, the cell-dense layer as well as the ventricular zone disappeared from the dorsal cord, and instead, cells in the dorsal horn showed a remarkable increase (Fig. 1*G*). In the ventral cord, the ventricular zone was found as a short neuroepithelial layer surrounding a narrow slit-like central canal (Fig. 1*G,H*). At this stage, cells with small dark nuclei appeared in the mantle and marginal zones, being scattered among neurons with large pale nuclei or nerve bundles, respectively (inset in Fig. 1*H*). At E18, the ventricular zone became a monolayer epithelium (ependymal layer) surrounding a small round central canal, except for the dorsalmost portion (Fig. 1*I,J*). Parallel with the histological reduction of the ventricular zone, the number of neuroepithelial cells was greatly reduced from E11 to E18; the mean nuclear profile number per single cross section was counted as 2887 ± 63 at E11, 640 ± 25 at E13, 112 ± 4 at E15, and 31 ± 1 at E18 (mean ± SEM; $n = 5$). On the contrary, the cell number in the mantle zone was prominently increased from E11 to E13; the mean nuclear profile number per single paraffin section was 776 ± 8 at E11, 2908 ± 42 at E13, 3102 ± 145 at E15, and 2831 ± 67 at E18 ($n = 5$). At P7, the floor plate disappeared, and the central canal was completely encircled by the ependymal layer, resulting in an adult-like appearance (Fig. 1*K*). After this, the size of the spinal cord increased slightly (Fig. 1*L*).

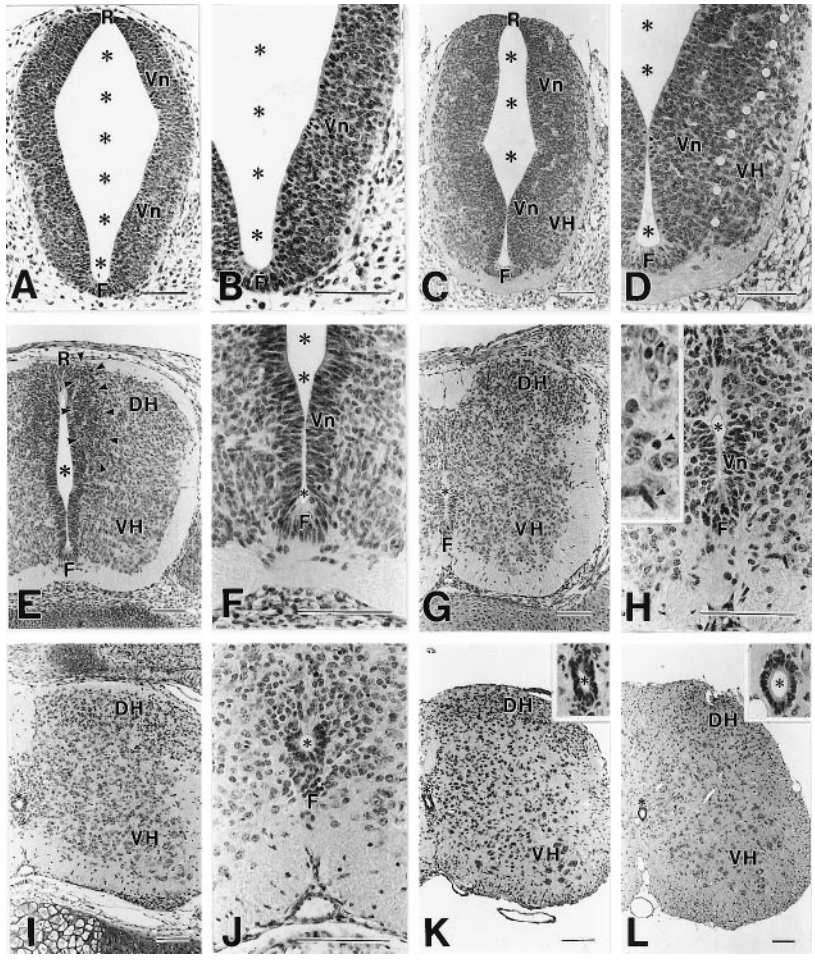

Figure 1. Histology of the developing spinal cord at E9 (*A, B*), E11 (*C, D*), E13 (*E, F*), E15 (*G, H*), E18 (*I, J*), P7 (*K*), and P21 (*L*). Hematoxylin-stained paraffin sections. *White circles* in *D* indicate the border between the ventricular zone (*Vn*) and ventral horn (*VH*). *Arrowheads* in *E* indicate a transient cell-dense layer formed between the ventricular zone and dorsal horn (*DH*). *Arrows* in *H* indicate putative glia cells with small dark nuclei. *F*, Floor plate; *R*, roof plate; *, central canal. Scale bars, 100 μm.

In situ hybridization

To clarify the cell position of GLAST-expressing cells, *in situ* hybridization was used in developing spinal cords, using ^{35}S-labeled antisense oligonucleotide probe (Fig. 2). At E11, low but significant signals were detected in the ventral half of the ventricular zone (Fig. 2*A*). At E13, GLAST mRNA was also confined to the ventricular zone, in which the ventral half including the floor plate was associated with higher signals than the dorsal half (Fig. 2*B*). At E15, prominent signals were observed in the ventricular zone and also in cells dispersed in the mantle zone (Fig. 2*C*). The GLAST mRNA-expressing cells in the mantle zone were distributed in proximity to the ventricular zone. From E18 to P7, signal levels in the ventricular zone were gradually reduced and disappeared, whereas a number of cells expressing GLAST mRNA spread all over the mantle zone (gray matter) and a few were distributed in the marginal zone (white matter) (Fig. 2*D–F*). Thereafter, the transcription levels were gradually decreased in various regions of the gray and white matters, and at the adult stage very faint signals were detectable only in the dorsal horn and around the central canal (Fig. 2*G*).

Characterization of anti-GLAST antibody

To characterize morphological and immunochemical properties of GLAST-expressing cells, affinity-purified anti-mouse GLAST antibody was raised in the rabbit and guinea pig. The specificity of antibodies was checked using the adult mouse brain, where the distribution of GLAST has been well characterized (Rothstein et al., 1994; Torp et al., 1994; Lehre et al., 1995). An immunoblot analysis showed that the rabbit antibody recognized heterogeneous protein bands at 60–65 kDa in membrane extracts from the adult mouse brain, showing a higher concentration in the cerebellum than in the forebrain (Fig. 3*A*). Immunohistochemistry with microslicer sections revealed a predominant distribution of GLAST in the molecular layer of the cerebellum, with lower levels in the telencephalon (Fig. 3*B*). In the preabsorption test, GLAST immunoreactivity decreased with the increase of antigen peptides added to the GLAST antibody; the immunoreactivity was completely abolished at the peptide concentration of 1 μg/ml in the telencephalon and at 10 μg/ml in the cerebellum (data not shown). The general distribution of GLAST immunoreactivity was consistent with that of GLAST mRNA (Fig. 3*C*). Similar results were obtained with the guinea pig antibody (data not shown). On the basis of these findings, these antibodies were judged to be specific to the glutamate transporter GLAST.

Immunohistochemistry

The spinal cord was examined by single-labeling (Figs. 4 and 5) and double-labeling (Fig. 6) immunohistochemistry. No immunoreactivity was detected at E9 (data not shown). At E11, GLAST immunoreactivity was detected in the ventral cord (Fig. 4*A*). Within the ventricular zone, higher levels were associated with the floor plate and ventricular side of the lateral wall. However, a narrow ventrobasal region adjacent to the floor plate lacked the immunoreactivity (*arrowheads* in Fig. 4*A*). Faint immunoreactivity was found in radially oriented fibrous processes and ran through the ventricular zone and ventral horn and reached the pial surface.

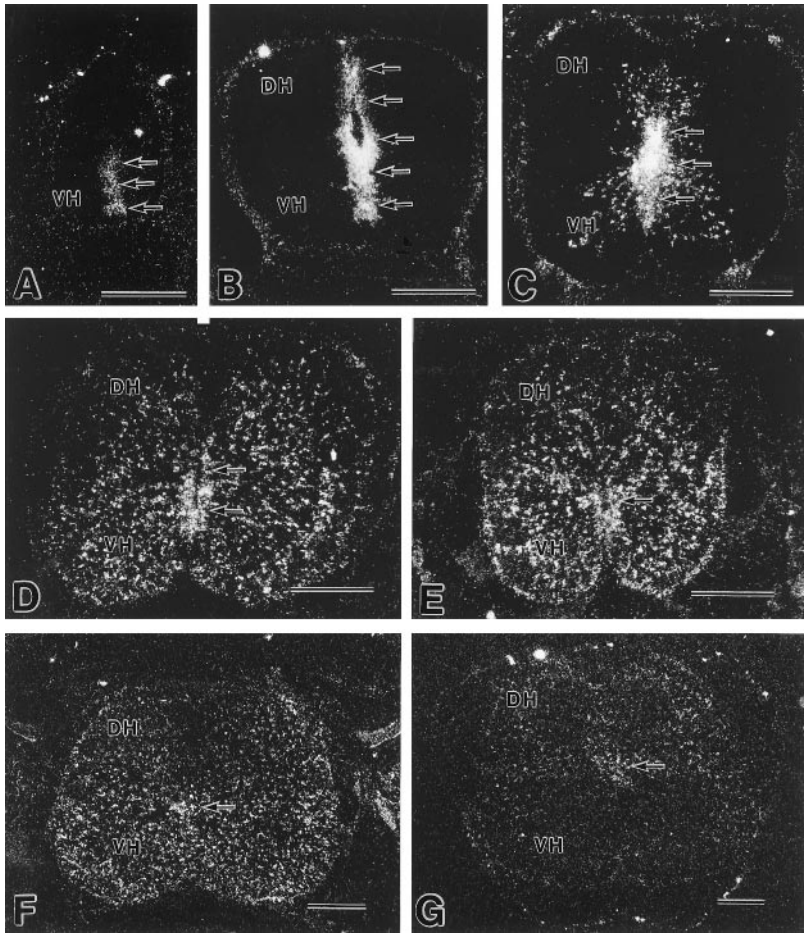

Figure 2. X-ray film autoradiography showing developmental changes of GLAST mRNA expression in the mouse spinal cord. *A*, E11; *B*, E13; *C*, E15; *D*, E18; *E*, P1; *F*, P7; *G*, adult. *Arrows* indicate position of the ventricular zone or the ependymal layer lining the central canal. *DH*, Dorsal horn; *VH*, ventral horn. Scale bars, 0.3 mm.

At E13, GLAST immunoreactivity prominently increased in the ventral cord, including the floor plate, ventricular zone, and radial processes (Fig. 4*B*). Radial processes gave off short circumferential branches between the mantle and marginal zones. In the dorsal cord, low immunoreactivity was detected in the ventricular zone and radial processes. The ventral cord at E13 was further examined by immunofluorescence with the GLAST antibody (as visualized with FITC, green) and by nuclear staining with propidium iodide (red) (Fig. 6*A*). GLAST immunoreactivity surrounded most of the cell bodies in the ventricular zone, which were elongated in shape and formed pseudostratified neuroepithelium. GLAST-immunopositive radial processes were smooth in contour and traversed the mantle zone between rows of GLAST-immunonegative neuronal cell bodies. When they reached the marginal zone, a cell-sparse region in the periphery, radial processes became rigid and terminated at the pial surface with conical (or deltoid) endfeet. Because GLAST is a cell membrane protein, its intracellular localization was compared with nestin, an intermediate filament contained in neuroepithelial cells at earlier fetal stages and in radial glia cells at later stages (Hockfield and McKay, 1985). By double immunofluorescence, GLAST-immunopositive radial processes (green) were also immunostained for nestin (red), but alternate color changes from yellow to green or red were seen in some portions (Fig. 6*B*). Moreover, nestin immunoreactivity was detected inside the endfoot of radial processes, whereas the GLAST antibody stained the margin (Fig. 6*B*).

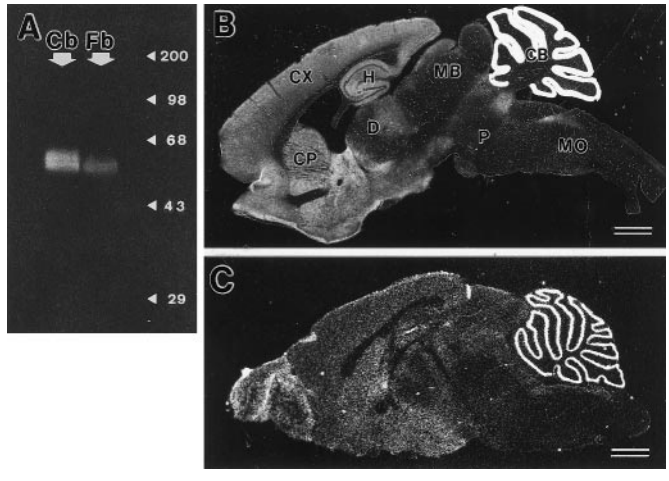

Figure 3. Characterization of rabbit anti-GLAST antibody. *A*, Immunoblot analysis. Crude membrane extracts from the cerebellum (*Cb*) and forebrain (*Fb*) of adult C57BL/6J mice were analyzed. The size of marker proteins is indicated to the *right* (kDa). *B*, Immunohistochemical analysis with parasagittal microslicer section through the adult mouse brain. *C, In situ* hybridization with parasagittal fresh frozen section through the adult mouse brain. Note a distribution of GLAST immunoreactivity similar to that of its mRNA. *CB*, Cerebellum; *CP*, caudate-putamen; *CX*, cerebral cortex; *D*, diencephalon; *H*, hippocampus; *MB*, midbrain; *MO*, medulla oblongata; *P*, pons. Rostral is to the *left*, and dorsal is to the *top*. Scale bars, 1 mm.

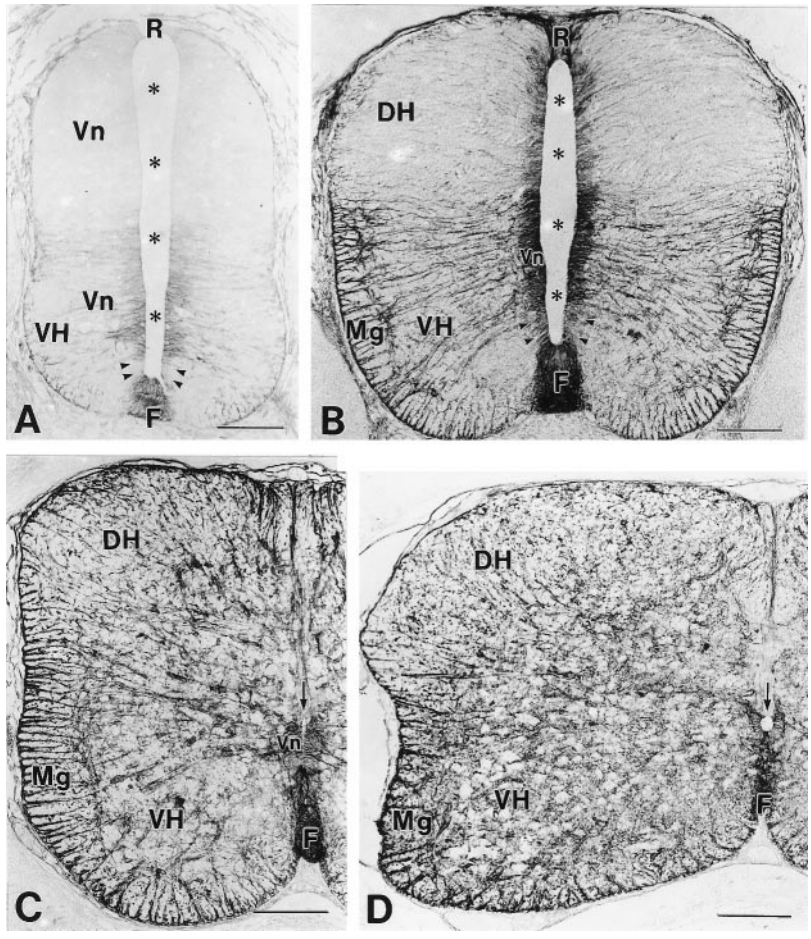

Figure 4. Immunohistochemical localization of GLAST in the fetal spinal cord. *A*, E11; *B*, E13; *C*, E15; *D*, E18. *Asterisks* and *arrows* indicate the central canal. *Arrowheads* in *A* and *B* indicate a ventrobasal region of the ventricular zone, which is associated with little or low GLAST immunoreactivity. *DH*, Dorsal horn; *F*, floor plate; *Mg*, marginal zone; *R*, roof plate; *VH*, ventral horn; *Vn*, ventricular zone. Scale bars, 100 μm.

At E15, GLAST immunoreactivity was lowered in the ventricular zone, whereas intense immunoreactivity was detected in the floor plate and in radial processes of both the ventral and dorsal cords (Fig. 4*C*). Between the radial processes, GLAST-immunopositive punctate or reticular structures were observed in the mantle and marginal zones. By double immunofluorescence, shafts of radial processes were labeled for both GLAST (green) and nestin (red) (Fig. 6*C,D*). When compared with E13, GLAST-immunopositive cell membrane at E15 was slightly dissociated from the nestin-immunopositive filaments (Fig. 6, *B* vs *D*). The punctate/reticular structures between radial processes were immunopositive for GLAST only and were often continuous with radial processes (*arrowheads* in Fig. 6*C,D*).

From E18 to P7, GLAST-immunoreactive punctate/reticular structures increased in number and predominated throughout the gray matter (mantle zone), whereas GLAST immunoreactivity was diminished or had disappeared from the floor plate, ventricular zone (ependymal layer), radial processes, and marginal zone (white matter) (Figs. 4*D*, 5*A,B*). To characterize the GLAST-expressing cells at P7, sections were double-labeled for GLAST mRNA and GFAP, an intermediate filament specific to astrocytes (Fig. 6*E*). A digoxigenin-labeled GLAST cRNA probe stained small cell bodies in the gray matter, but not large neuronal ones. From the labeled cell bodies, GFAP-immunopositive short fibers extended in various directions (Fig. 6*E*). Double immunofluorescence for GLAST and GFAP showed that GLAST-immunopositive punctate/reticular structures were distributed around GFAP-immunopositive fibers, showing little overlap (Fig. 6*F*). Using antibody against synaptophysin, a synaptic vesicle protein, these GLAST-immunopositive punctate/reticular structures were shown to be apposed closely to nerve terminals (Fig. 6*G*).

At P14 and P21, the GLAST immunoreactivity displayed a remarkable increase in neuropil regions throughout the gray matter, in which GLAST-immunonegative neuronal cell bodies and thick dendrites were observed as pale silhouettes (Fig. 5*C,D*). Thereafter, the immunoreactivity decreased substantially, and only low to moderate levels were detected in superficial layers of the dorsal horn and around the central canal in the adult stage (Fig. 5*E*), consistent with a previous report (Lehre et al., 1995).

DISCUSSION

GLAST is expressed in radial glia–astrocyte lineage

Radial glia cells are a distinct cell class of the neuroglia. At early stages, the cell bodies are located in the ventricular or subventricular zone, and their long radial processes span the neural tube, ending at the pial surface or blood vessels with conical endfeet (Ramón y Cajal, 1911; Rakic, 1971a, 1972; Choi, 1981; Gressens et al., 1992). Radial glia cells exist transiently at neurogenesis and neuronal migration, and they migrate and transform into astrocytes. Expressions of intermediate filaments also exhibit developmental changes; in various nonprimate mammals, vimentin, nestin (Rat-401 antigen), and RC1 and RC2 antigens constitute intermediate filaments or filament-related antigens in radial glia cells and immature astrocytes, whereas GFAP is predominant in mature astrocytes (Schnitzer et al., 1981; Bignami et al., 1982; Bovolenta et al., 1984; Pixley and de Vellis, 1984; Hockfield and

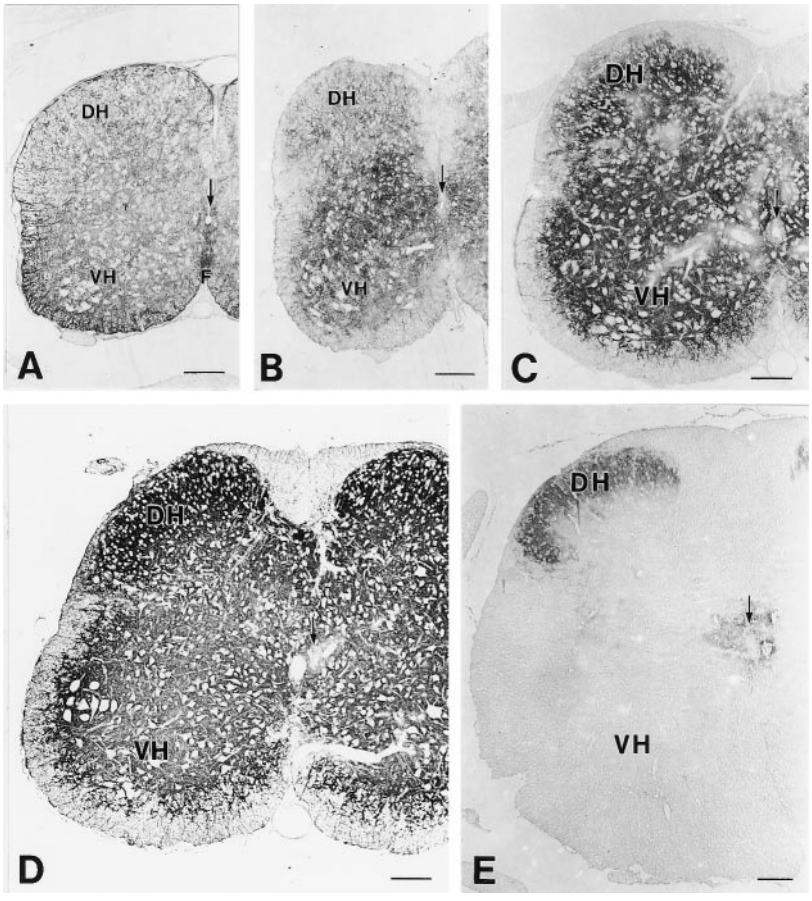

Figure 5. Immunohistochemical localization of GLAST in the postnatal spinal cord. *A*, P1; *B*, P7; *C*, P14; *D*, P21; *E*, adult. Note strong GLAST immunoreactivity throughout the gray matter at P14 and P21, whereas it disappears from most regions of the gray matter at the adult stage. *Arrows* indicate the ependymal layer lining the central canal. *DH*, Dorsal horn; *F*, floor plate; *VH*, ventral horn. Scale bars, 100 μm.

McKay, 1985; McDermott and Lantos, 1989; Voigt, 1989; Edwards et al., 1990; Ghooray and Martin, 1993). In this study at E11 and E13, cells expressing GLAST were localized in the ventricular zone and displayed such cytological characteristics of the radial glia cells. At P7, GLAST mRNA was expressed in GFAP-immunopositive astrocytes, and GLAST immunoreactivity was observed as synapse-associated punctate/reticular structures in the gray matter. Between these two stages, the immunoreactivity was detected in both the radial processes and punctate/reticular structures. Therefore, it is reasonable to judge that GLAST is expressed from radial glia cells through astrocytes in the mouse spinal cord. The present study has also shown that the localization restricted to the dorsal horn and around the central canal at the adult stage is established through downregulation in mature astrocytes.

GLAST appears on radial glia cells during neuronal migration

Spinal cord neurons are generated at early stages (Fujita, 1964; Nornes and Das, 1974; Sims and Vaughn, 1979; Altman and Bayer, 1984). According to Sims and Vaughn (1979), lateral motor neurons in the mouse cervical cord are mostly generated between E9 and E10.5, and dorsal horn neurons in the laminae I–III are born at about E12. Radial glia cells are present from the stage of neurogenesis, as shown by Golgi technique and by immunohistochemistry (Choi, 1981; Hockfield and McKay, 1985; Edwards et al., 1990). For example, RC1 antibody stains radial glia cells in the mouse spinal cord as early as E9, and RC1-immunopositive radial processes span the ventral and dorsal cords at E12 (Edwards et al., 1990). When compared with the previous radial glial cell markers, the appearance of GLAST immunoreactivity is relatively late and shows a distinct ventral-to-dorsal gradient. In the ventral cord, GLAST immunoreactivity was first detected at E11, when a small ventral horn begins to be formed. It became intense by E13, when the ventral horn had become enlarged and contained a number of neuronal cell bodies. In the dorsal cord, GLAST immunoreactivity appeared at E13 and became intense at E15, during which period cells in the dorsal horn increased in number. Therefore, the GLAST appears on preexisting radial glia cells at stages when spinal cord neurons migrate from the ventricular zone to the mantle zone.

Radial glial cells migrate after neuronal migration

By ^{3}H-thymidine autoradiography and Feulgen cytophotometry, Fujita (1965, 1973) has shown that DNA synthesizing cells first appear in the mantle and marginal zones at the 8 week stage in the human spinal cord and at the 8 d stage in the chick spinal cord. In the human spinal cord at the 7.5 week stage, cell bodies of radial glia cells begin to be displaced from the wall of the ventricular zone (Choi, 1981). In the present study, we observed that cells expressing GLAST mRNA first emerged outside the ventricular zone at E15. At this stage, glia-like cells, which contain small nuclei stained heavily with hematoxylin, were distinguished in the mantle and marginal zones. All of these findings suggest that radial glia cells retaining mitotic activities begin to migrate at a specific stage of development. In the mouse spinal cord, the migration begins between E13 and E15. On the other hand, a substantial number of neuroepithelial cells were lost from the ventricular zone between E11 and E13, when cells in the ventral and dorsal horns had increased, representing a massive

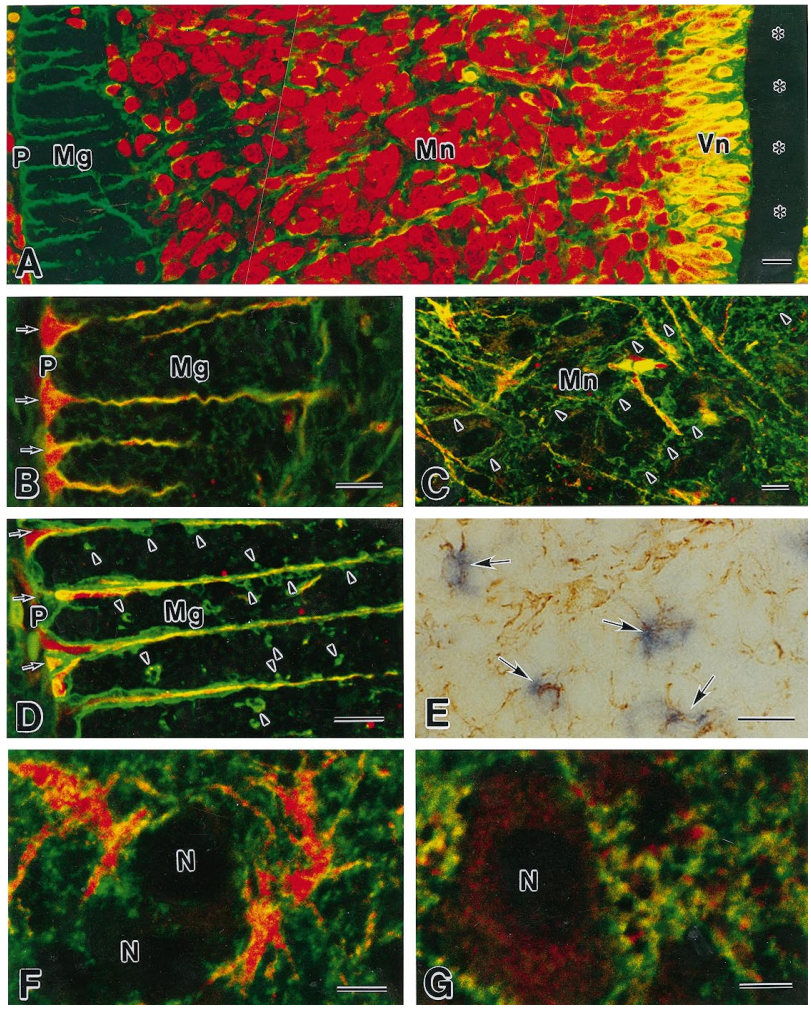

Figure 6. Double-labeling showing morphological and immunochemical properties of GLAST-expressing cells at E13 (*A, B*), E15 (*C, D*), and P7 (*E–G*). *A*, GLAST immunoreactivity (*green*) and nuclear staining with propidium iodide (*red*). *B–D*, GLAST immunoreactivity (*green*) and nestin immunoreactivity (*red*) in the marginal zone (*B, D*) and mantle zone (*C*). *Arrowheads* indicate GLAST-immunopositive punctate or irregular protrusions from radial processes. *Arrows* indicate conical endfeet of radial processes. *E*, GLAST mRNA (*purple*) and GFAP immunoreactivity (*brown*). *Arrows* indicate cell bodies labeled for the GLAST mRNA. *F*, GLAST immunoreactivity (*green*) and GFAP immunoreactivity (*red*). *G*, GLAST immunoreactivity (*green*) and synaptophysin immunoreactivity (*red*). *Mg*, Marginal zone; *Mn*, mantle zone; *N*, neuronal cell body; *P*, pial surface; *Vn*, ventricular zone; *, central canal. Scale bars, *A–D*, *F*, 10 μm; *E*, 50 μm; *G*, 5 μm.

neuronal migration. Therefore, the migration of radial glia cells occurs after active neuronal migration.

Concomitant transformation and migration of radial glia cells

By taking advantage of the cell membrane localization, immunohistochemistry for GLAST enabled visualization of cytological changes of radial glia cells. Radial glial processes were smooth in contour at E13, whereas a number of punctate/reticular protrusions were formed at E15 along or between radial processes. The latter structures gradually increased and predominated in the gray matter at early postnatal stages. Therefore, the cytological change between E13 and E15 represents an initial sign of the radial glial transformation. Thus, it seems likely that the transformation and migration of radial glia cells occur concomitantly. This is consistent with a previous finding from Golgi studies in which numerous lamellate expansions appear along radial processes at the stage when the cell bodies begin to be displaced from the ventricular zone (Schmechel and Rakic, 1979; Choi, 1981).

Speculated roles of GLAST on radial glia cells

Mature astrocytes surround various structures in the CNS, including synapses, dendritic shafts, neuronal cell bodies, capillaries, and pia mater. Dense localization on astrocytic membrane apposing synapses is demonstrated for GLAST and also for GLT1, another glutamate transporter expressed in astrocytes (Chaudhry et al., 1995). The extracellular glutamate concentration is elevated in rats infused intraventricularly with GLAST or GLT1 antisense oligonucleotide (Rothstein et al., 1996). Mice defective in GLT1 display prolonged high glutamate levels in the synaptic cleft, epilepsy, and neuronal cell death (Tanaka K et al., 1997). It is thus clear that glutamate transporters on mature astrocytes play an essential role in the rapid removal of extracellular glutamate, to keep the level low enough to prevent neurons from excitotoxicity. What can be speculated as a role of GLAST on radial glia cells?

Radial glia cells are thought to serve as a guide for neuronal migration (Rakic, 1971a, 1972; Gregory et al., 1988). In the developing cerebellum, migrating granule cells are directly apposed to Bergmann glial fibers (Rakic, 1971b). Komuro and Rakic (1993) have shown using slice preparations that the rate of granule cell migration is increased by the activation of NMDA receptor channels. Because synapses are not yet differentiated in migrating granule cells, the cell migration is facilitated by activation of nonsynaptic NMDA receptor channels. Interestingly, the cell migration is also accelerated by the administration of the glutamate uptake inhibitor *p*-chloromercuriphenylsulfonic acid (Komuro and Rakic, 1993). In this regard, the dense localization of GLAST on radial glial processes seems to be of great interest, in terms of regulation of the glutamate level along the course of migrating neurons. If GLAST on radial glial processes lowers the glutamate level, it would slow the neuronal migration and protect migrating neurons from excessive receptor activation leading to excitotoxicity. Alternatively, if GLAST supplies glutamate to

migrating neurons, it would facilitate the migration. It has been postulated that early in development the reversed transporter operation from intracellular to extracellular space is the source of neurotransmitters (Taylor and Gordon-Weeks, 1991). It should also be taken into consideration that GLAST is involved in differentiation of the radial glia–astrocyte lineage. In the future, developmental analyses of mice lacking GLAST will provide an important insight into its role in neural development.

REFERENCES

Altman J, Bayer SA (1984) The development of the rat spinal cord. Adv Anat Embryol Cell Biol 85:1–168.

Bignami A, Raju T, Dahl D (1982) Localization of vimentin, the nonspecific intermediate filament protein, in embryonal glia and in early differentiating neurons. In vivo and in vitro immunofluorescence study of the rat embryo with vimentin and neurofilament antisera. Dev Biol 91:286–295.

Bovolenta P, Liem RKH, Mason CA (1984) Development of cerebellar astroglia: transitions in form and cytoskeletal content. Dev Biol 102:248–259.

Chaudhry FA, Lehre KP, Campagne ML, Ottersen OP, Danbolt NC, Storm-Mathisen J (1995) Glutamate transporters in glial plasma membranes: highly differentiated localizations revealed by quantitative ultrastructural immunocytochemistry. Neuron 15:711–720.

Choi BH (1981) Radial glia of developing human fetal spinal cord: Golgi, immunohistochemical and electron microscopic study. Dev Brain Res 1:249–267.

Choi DW (1992) Excitotoxic cell death. J Neurobiol 23:1261–1276.

Edwards MA, Yamamoto M, Caviness Jr VS (1990) Organization of radial glia and related cells in the developing murine CNS. An analysis based upon a new monoclonal antibody marker. Neuroscience 36:121–144.

Fujita S (1964) Analysis of neuron differentiation in the central nervous system by tritiated thymidine autoradiography. J Comp Neurol 122:311–328.

Fujita S (1965) An autoradiographic study on the origin and fate of the sub-pial glioblast in the embryonic chick spinal cord. J Comp Neurol 124:41–60.

Fujita S (1973) Genesis of glioblasts in the human spinal cord as revealed by Feulgen cytophotometry. J Comp Neurol 151:25–34.

Ghooray GT, Martin G (1993) Development of radial glia and astrocytes in the spinal cord of the North American opossum (*Didelphis virginiana*): an immunohistochemical study using anti-vimentin and anti-glial fibrillary acidic protein. Glia 9:1–9.

Gregory WA, Edmondson JC, Hatten ME, Mason CA (1988) Cytology and neuron-glial apposition of migrating cerebellar granule cells in vitro. J Neurosci 8:1728–1738.

Gressens P, Richelme C, Kadhim HJ, Gadisseux J-F, Evrard P (1992) The germinative zone produces the most cortical astrocytes after neuronal migration in the developing mammalian brain. Biol Neonate 61:4–24.

Hertz L (1979) Functional interactions between neurons and astrocytes. I. Turnover and metabolism of putative amino acid transmitters. Prog Neurobiol 13:277–323.

Hockfield S, McKay RD (1985) Identification of major cell classes in the developing mammalian nervous system. J Neurosci 5:3310–3328.

Kanai Y, Hediger MA (1992) Primary structure and functional characterization of a high-affinity glutamate transporter. Nature 360:467–471.

Kanai Y, Bhide PG, DiFiglia M, Hediger MA (1995) Neuronal high-affinity glutamate transport in the rat central nervous system. NeuroReport 6:2357–2362.

Kanai Y, Trotti D, Nussberger S, Hediger MA (1997) The high affinity glutamate transporter family: structure, function, and physiological relevance. In: Neurotransmitter transporters. Structure, function, and regulation (Reith MEA, ed), pp 171–213. Totowa, NJ: Humana.

Kiryu S, Yao GL, Morita N, Kato H, Kiyama H (1995) Nerve injury enhances rat neuronal glutamate transporter expression: identification by differential display PCR. J Neurosci 15:7872–7878.

Komuro H, Rakic P (1993) Modulation of neuronal migration by NMDA receptors. Science 260:95–98.

Lehre KP, Levy LM, Ottersen OP, Storm-Mathisen J, Danbolt NC (1995) Differential expression of two glial glutamate transporters in the rat brain: quantitative and immunocytochemical observations. J Neurosci 15:1835–1853.

Mayer BL, Westbrook GL (1987) The physiology of excitatory amino acids in the vertebrate central nervous system. Prog Neurobiol 28:197–276.

McDermott KWG, Lantos PL (1989) The distribution of glial fibrillary acidic protein and vimentin in postnatal marmoset (*Callithrix jacchus*) brain. Dev Brain Res 45:169–177.

Nornes HO, Das GD (1974) Temporal patter of neurogenesis in spinal cord of rat. I. An autoradiographic study-time and sites of origin and migration and settling patterns of neuroblasts. Brain Res 73:121–138.

Pixley SR, de Vellis J (1984) Transition between immature radial glia and mature astrocytes studied with a monoclonal antibody to vimentin. Dev Brain Res 15:201–209.

Rakic P (1971a) Guidance of neurons migrating to the fetal monkey neocortex. Brain Res 33:471–476.

Rakic P (1971b) Neuron-glia relationship during granule cell migration in developing cerebellar cortex. A Golgi and electronmicroscopic study in Macacus rhesus. J Comp Neurol 141:293–312.

Rakic P (1972) Mode of cell migration to the superficial layers of fetal monkey neocortex. J Comp Neurol 145:61–84.

Ramón y Cajal S (1911) Histologie du Systeme Nerveux de l'Homme et des Vertébrés. Tome 2. Paris Maloine. Reprinted by Consejo Superior de Investigaciones Cientificas: Madrid, 1955.

Rothstein JD, Martin L, Levey AI, Dykes-Hoberg M, Jin L, Wu D, Nash N, Kuncl RW (1994) Localization of neuronal and glial glutamate transporters. Neuron 13:713–725.

Rothstein JD, Dykes-Hoberg M, Pardo CA, Bristol LA, Jin L, Kuncl RW, Kanai Y, Hediger MA, Wang Y, Schielke JP, Welty DF (1996) Knockout of glutamate transporters reveals a major role for astroglial transport in excitotoxicity and clearance of glutamate. Neuron 16:675–686.

Schmechel DE, Rakic P (1979) A Golgi study of radial glial cells in developing monkey telencephalon: morphogenesis and transformation into astrocytes. Anat Embryol 156:115–152.

Schnitzer J, Franke WW, Schachner M (1981) Immunocytochemical demonstration of vimentin in astrocytes and ependymal cells of developing and adult mouse nervous system. J Cell Biol 90:435–447.

Shibata T, Watanabe M, Tanaka K, Wada K, Inoue Y (1996) Dynamic changes in expression of glutamate transporter mRNAs in developing brain. NeuroReport 7:705–709.

Sims TJ, Vaughn JE (1979) The generation of neurons involved in an early reflex pathway of embryonic mouse spinal cord. J Comp Neurol 183:707–720.

Storck T, Schulte S, Hofmann K, Stoffel W (1992) Structure, expression, and functional analysis of a Na^+-dependent glutamate/aspartate transporter from rat brain. Proc Natl Acad Sci USA 89:10955–10959.

Sutherland ML, Delaney TA, Noebels JL (1996) Glutamate transporter mRNA expression in proliferative zones of the developing and adult murine CNS. J Neurosci 16:2191–2207.

Tanaka K (1993) Cloning and expression of a glutamate transporter from mouse brain. Neurosci Lett 159:183–186.

Tanaka J, Ichikawa R, Watanabe M, Tanaka K, Inoue Y (1997) Extrajunctional localization of glutamate transporter EAAT4 at excitatory Purkinje cell synapses. NeuroReport 8:2461–2464.

Tanaka K, Watase K, Manabe T, Yamada K, Watanabe M, Takahasi K, Iwama H, Nishikawa T, Ichihara N, Kikuchi T, Okuyama S, Kawashima N, Hori S, Takimoto M, Wada K (1997) Epilepsy and exacerbation of brain injury in mice lacking the glutamate transporter GLT-1. Science 276:1699–1702.

Taylor J, Gordon-Weeks P (1991) Calcium-independent gamma-aminobutyric acid release from growth cones: role of gamma-aminobutyric acid transporter. J Neurochem 56:273–280.

Tomooka Y, Kitani H, Jing N, Matsubara M, Sakakura T (1993) Reconstruction of neural tube-like structures in vitro from primary neural precursor cells. Proc Natl Acad Sci USA 90:9683–9687.

Torp R, Danbolt NC, Babaie E, Bjørås M, Seeberg, E, Storm-Mathisen J, Ottersen OP (1994) Differential expression of two glial glutamate transporters in the rat brain: an *in situ* hybridization study. Eur J Neurosci 6:936–942.

Voigt T (1989) Development of glial cells in the cerebral wall of ferrets: direct tracing of their transformation from radial glia into astrocytes. J Comp Neurol 289:74–88.

Yamada K, Watanabe M, Shibata T, Tanaka K, Wada K, Inoue Y (1996) EAAT4 is a post-synaptic glutamate transporter at Purkinje cell synapses. NeuroReport 7:2013–2017.

Yamada K, Wada S, Watanabe M, Tanaka K, Wada K, Inoue Y (1997) Changes in expression and distribution of the glutamate transporter EAAT4 in developing mouse Purkinje cells. Neurosci Res 27:191–198.